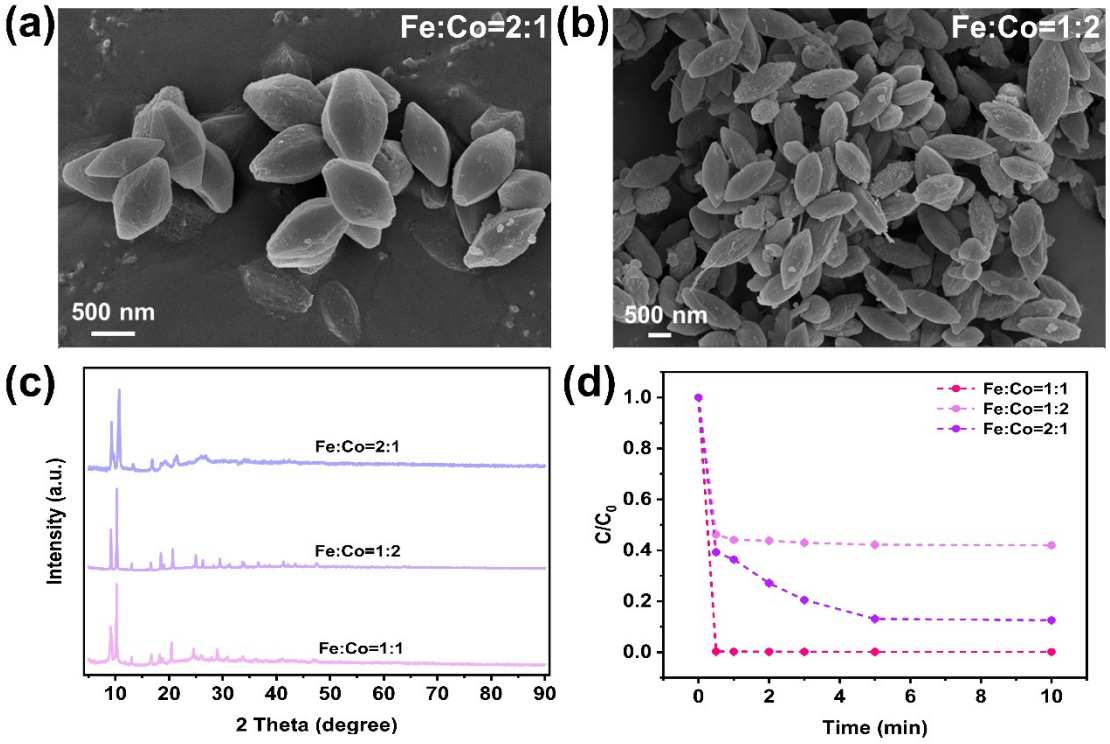

Fig. S1 SEM images of MIL-101(CoFe)-NH_2 prepared with Fe:Co precursor feeding ratios of 2:1 (a) and 1:2 (b); XRD patterns (c) and degradation performance (d) of MIL-101(CoFe)-NH_2 samples prepared with different Fe:Co precursor feeding ratios

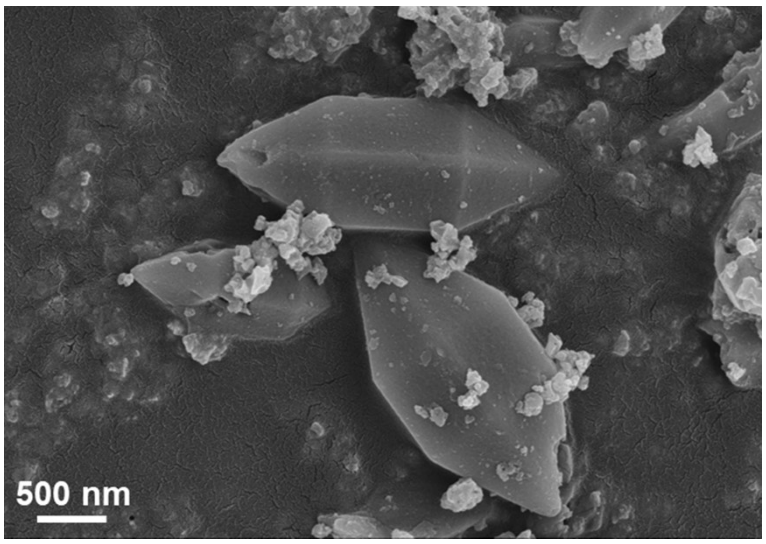

Fig. S2 SEM image of MIL-101(Fe)-NH_2

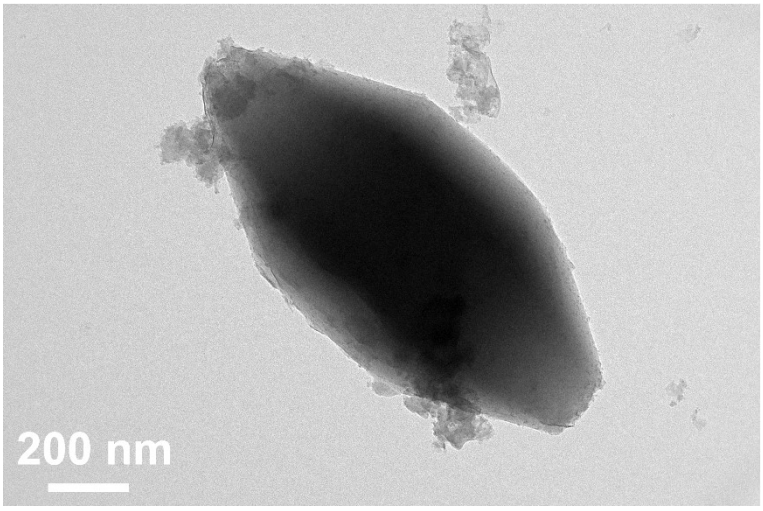

Fig. S3 TEM image of MIL-101(CoFe)-NH_2

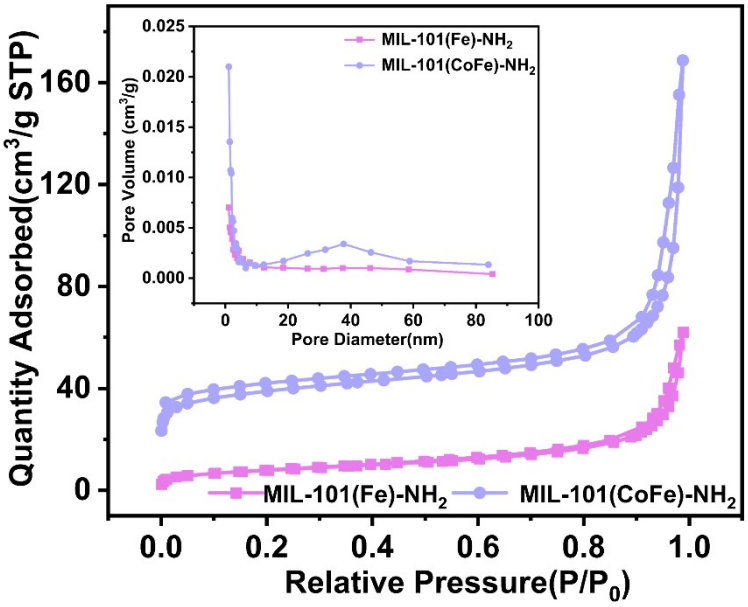

Fig. S4 BET diagrams of MIL-101(Fe)-NH_2 and MIL-101(CoFe)-NH_2 materials

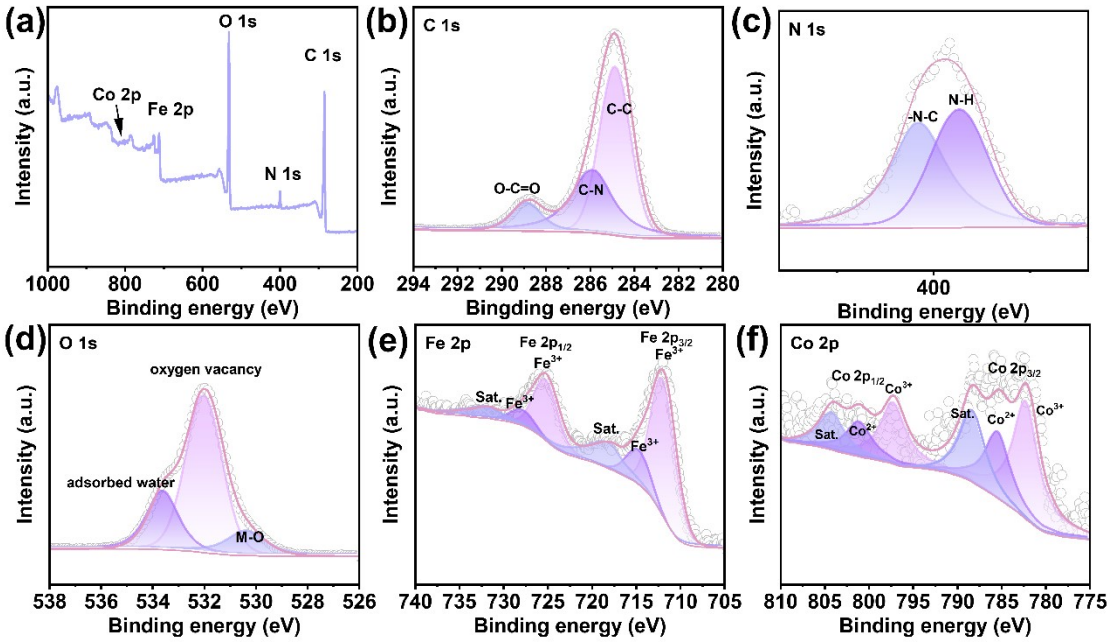

Fig. S5 XPS spectra of MIL-101(CoFe)-NH_2: survey spectrum (a), C 1s (b), N 1s (c), O 1s (d), Fe 2p (e) and Co 2p (f)

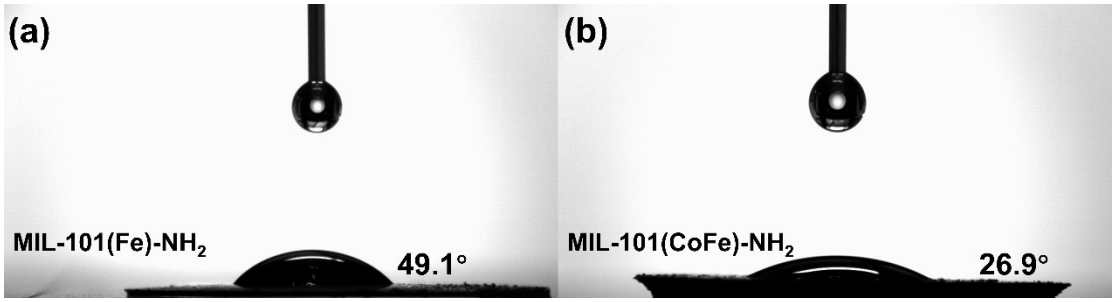

Fig. S6 Contact angles of MIL-101(Fe)-NH_2 (a) and MIL-101(CoFe)-NH_2 (b)

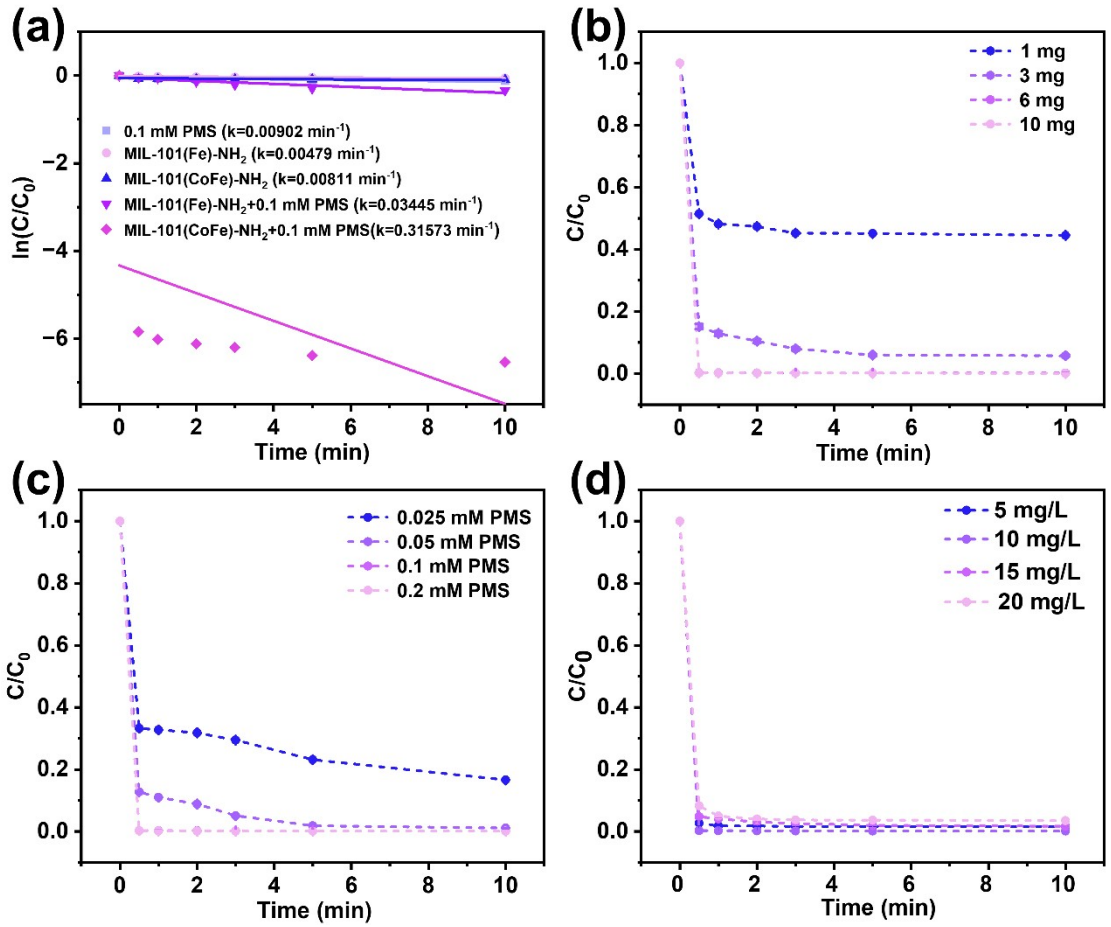

Fig. S7 Pseudo-first-order kinetic fitting plots of degradation performance of various catalysts (a); Effects of different conditions on the degradation of SDZ by MIL-101(CoFe)-NH_2: catalyst dosage (b), PMS dosage (c), and pollutant concentration (d)

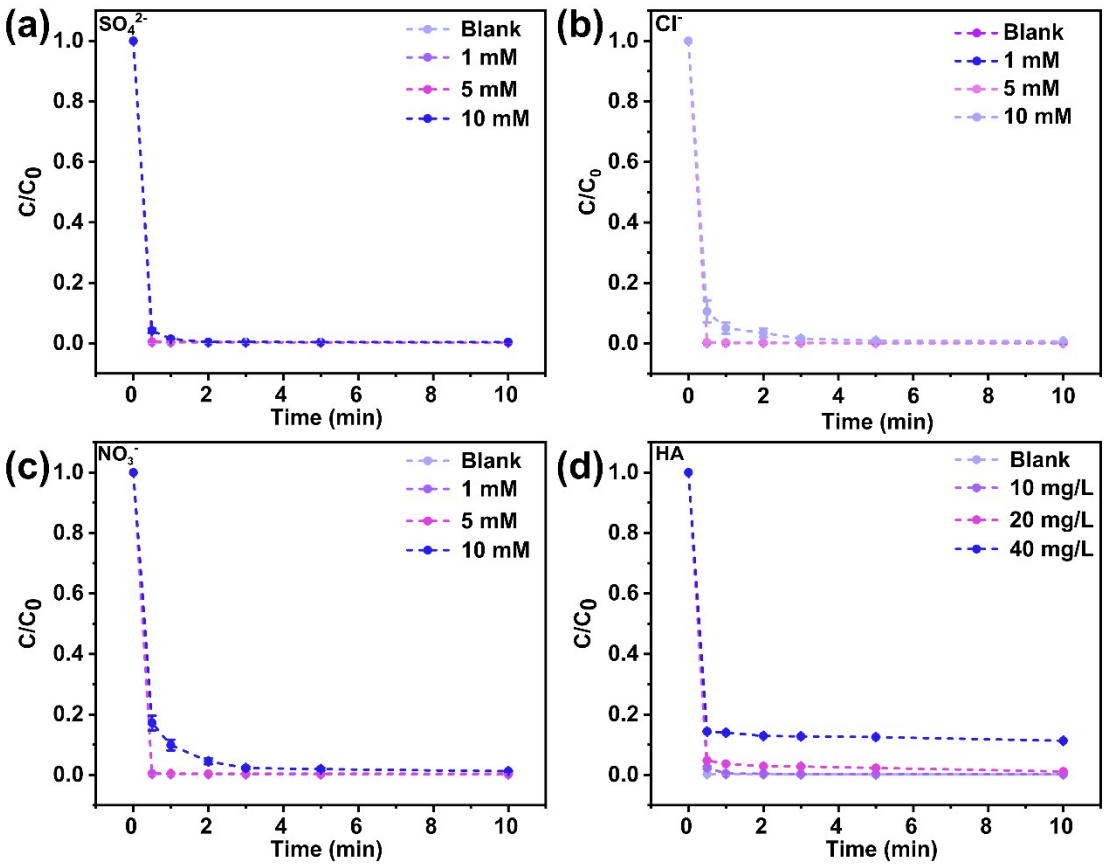

Fig. S8 Effect of coexisting ions and humic acid on the degradation of SDZ by MIL-101(CoFe)-NH_2: SO_4^{2-} (a), Cl^- (b), NO_3^- (c) and HA (d)

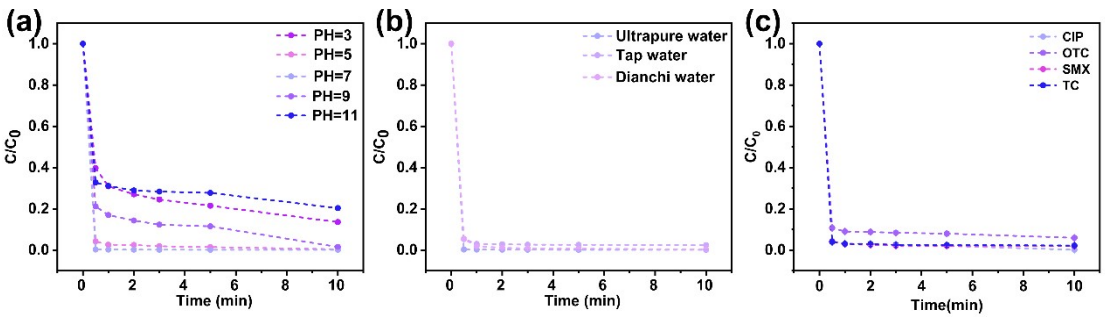

Fig. S9 Effect of different pH (a) and different experimental water bodies (b) on the degradation of SDZ by MIL-101(CoFe)-NH_2; Removal ability of MIL-101(CoFe)-NH_2 catalyst for different antibiotics (c)

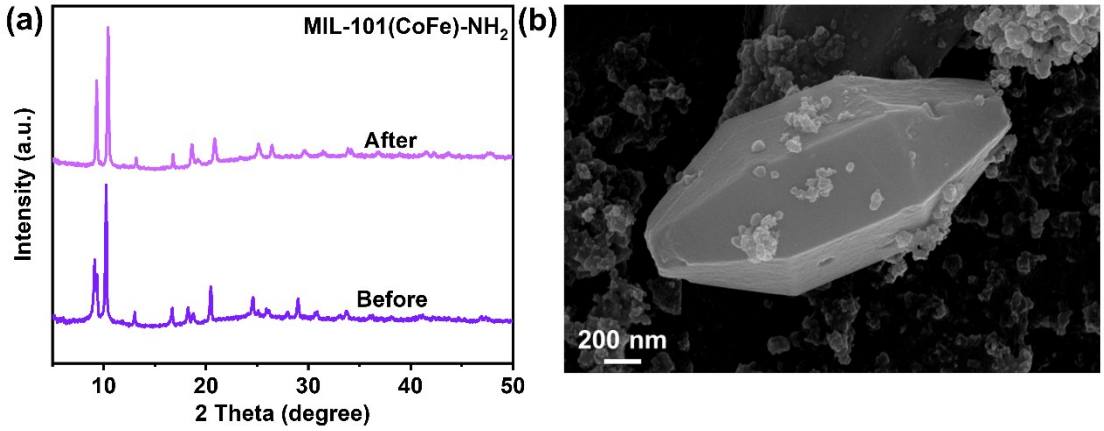

Fig. S10 XRD and SEM of MIL-101(CoFe)-NH_2 after cycling

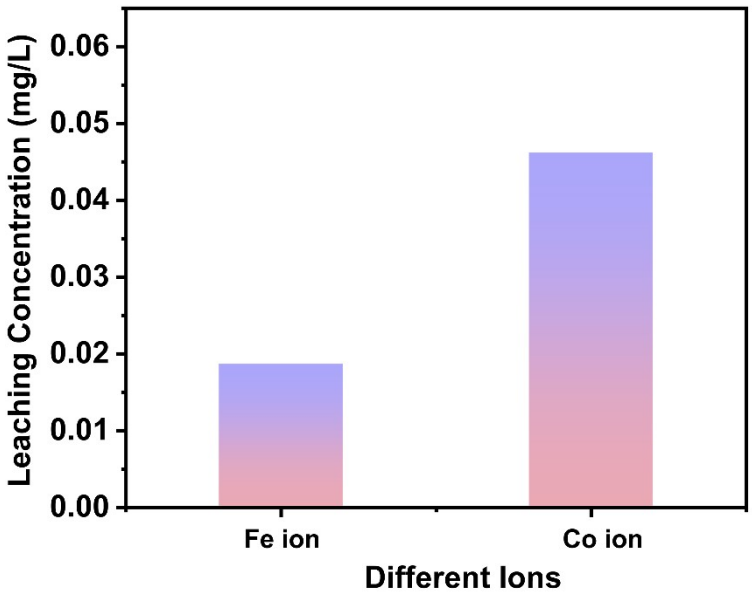

Fig. S11 Leaching concentration of Fe and Co ions

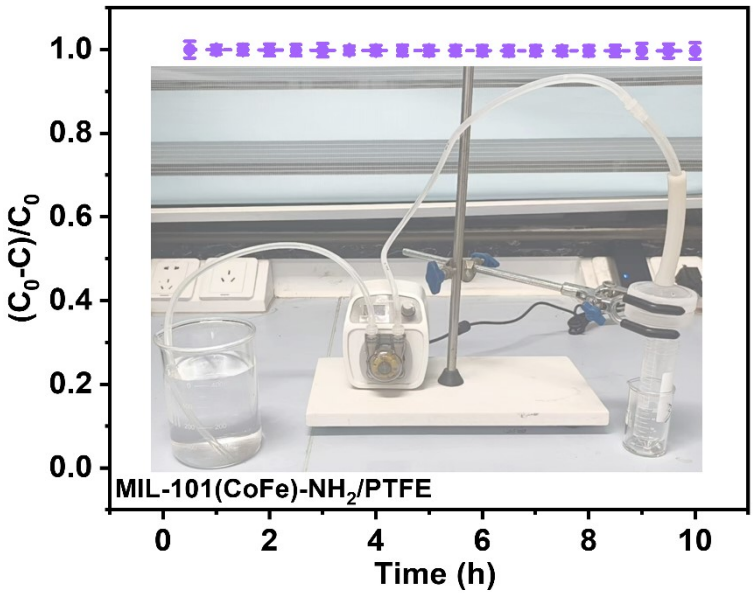

Fig. S12 Continuous flow degradation diagram of MIL-101(CoFe)-NH_2/PTFE membrane

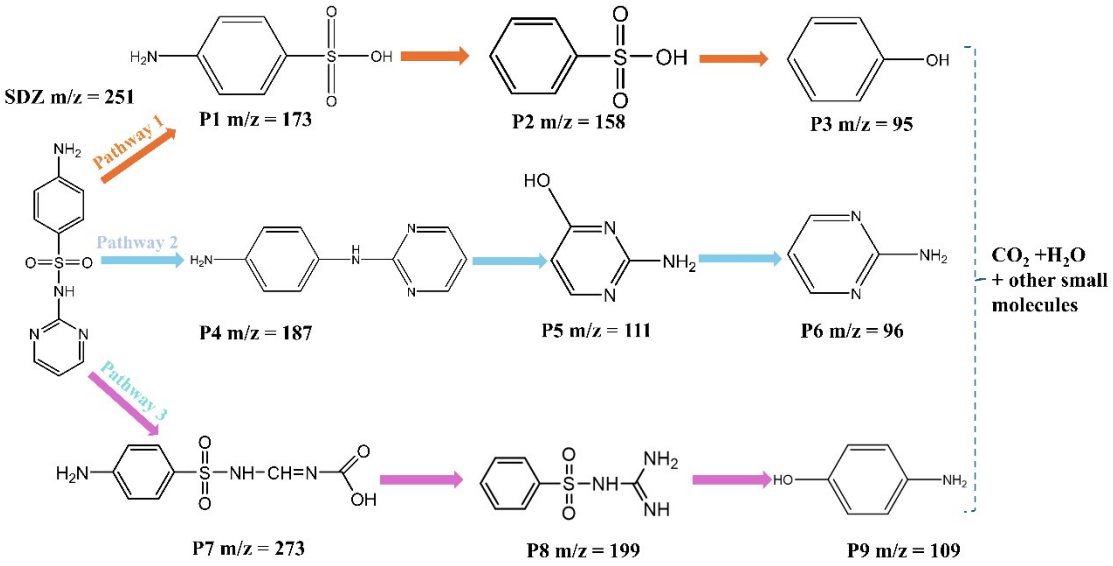

Fig. S13 Possible reaction pathways of SDZ degradation in the MIL-101(CoFe)-NH_2/PMS system

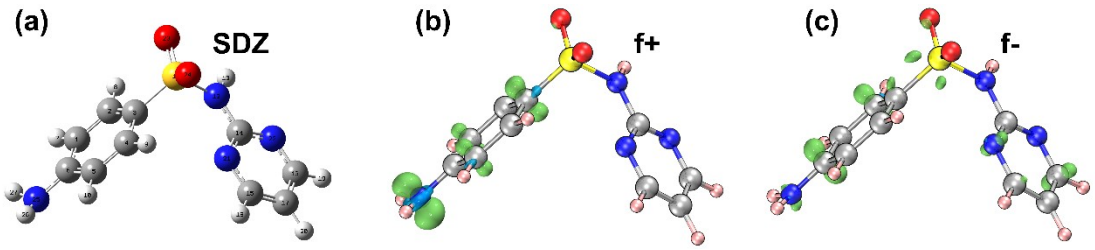

Fig. S14 SDZ molecular structure (a), SDZ Fukui function (f^+) (b) and SDZ Fukui function (f^-) (c) in the MIL-101(CoFe)-NH_2/PMS system

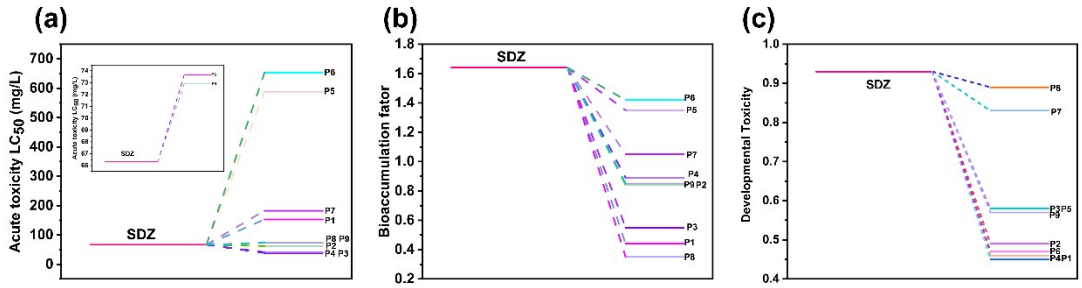

Fig. S15 Acute toxicity (a), bioaccumulation factor (b), and developmental toxicity (c) of different degradation products

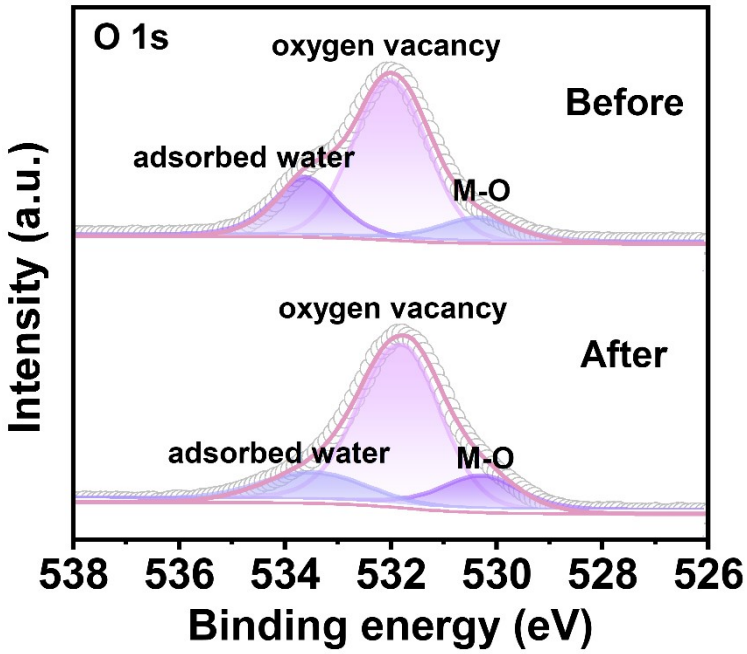

Fig. S16 XPS spectra of O 1s for MIL-101(CoFe)-NH_2 before and after the reaction

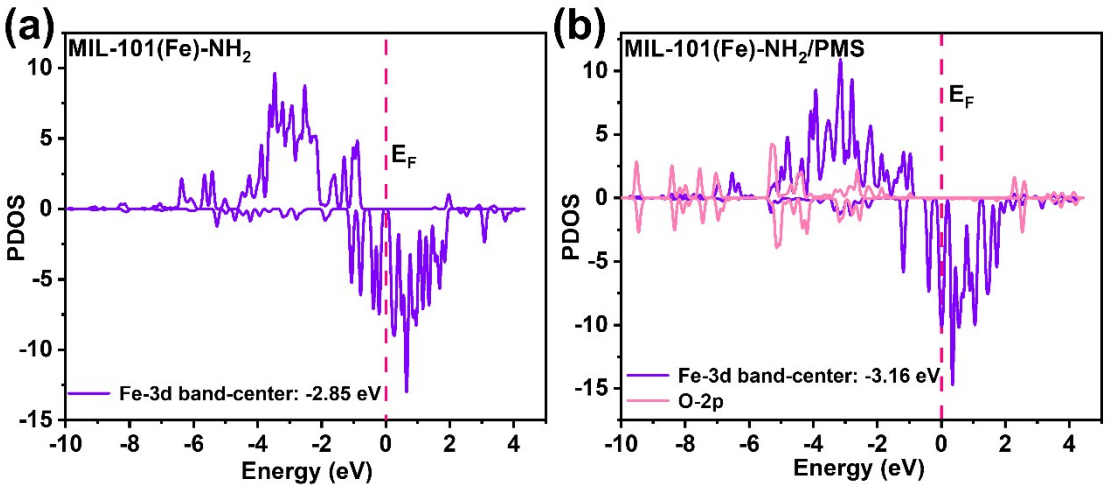

Fig. S17 The density of states of MIL-101(Fe)-NH_2 and the adsorbed PMS

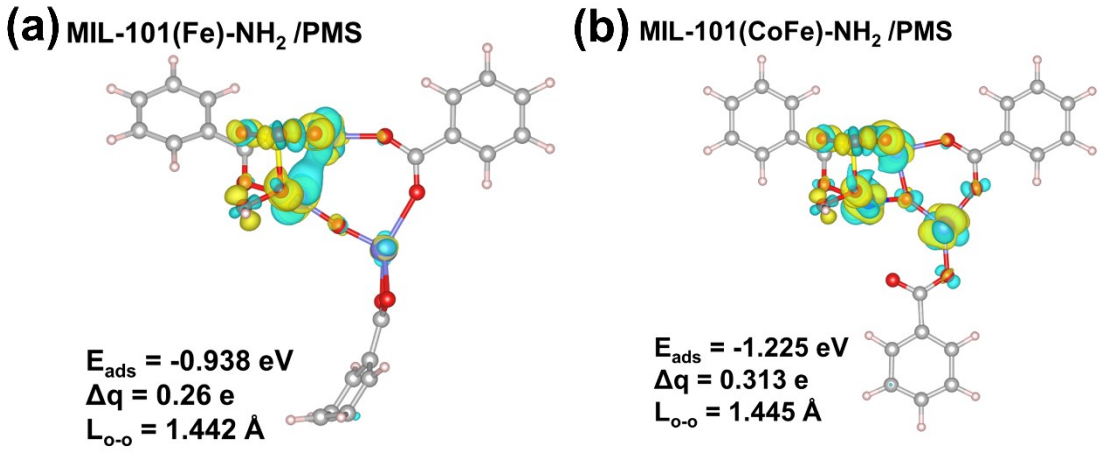

Fig. S18 The differential charge density of adsorbed PMS

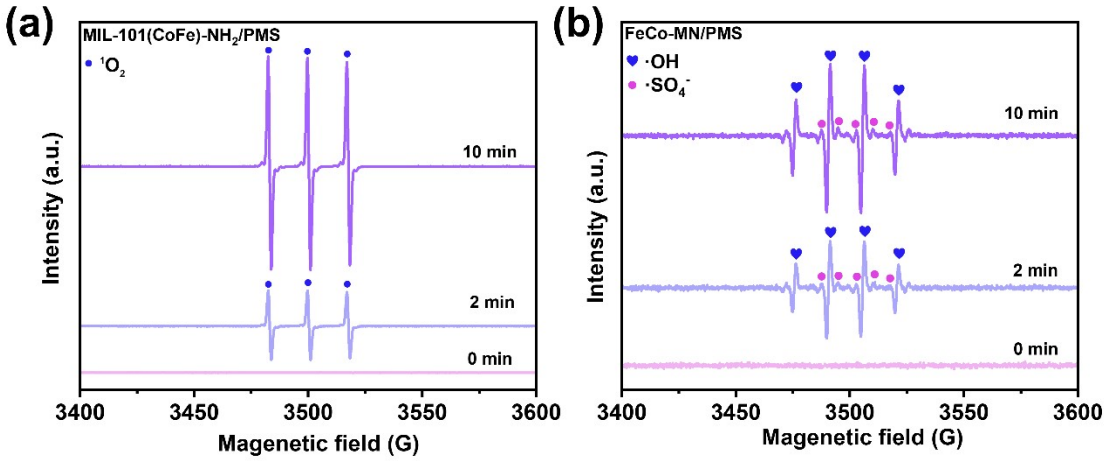

Fig. S19 TEMP-$^1O_2$ test (a) and DMPO-·OH and $\cdot SO_4^-$ tests (b) of MIL-101(CoFe)-NH_2

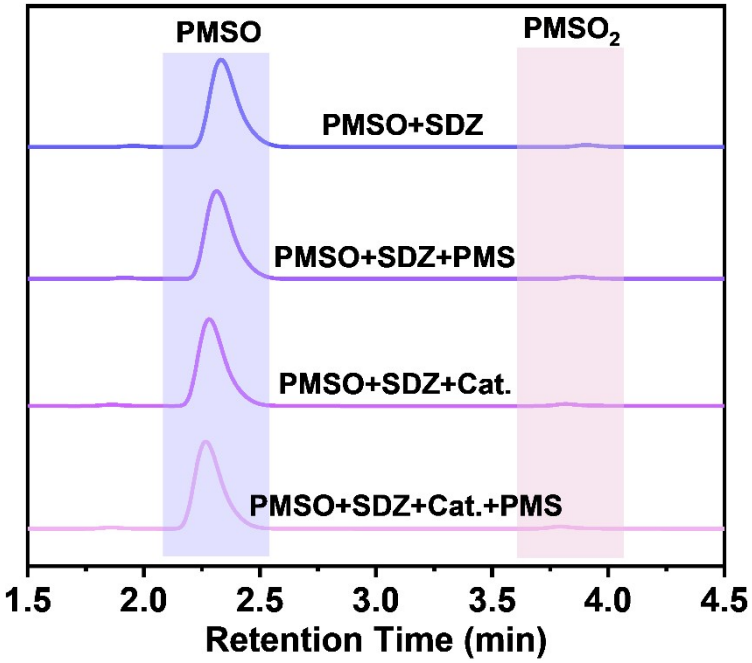

Fig. S20 PMSO-high-valent metal species test of MIL-101(CoFe)-NH_2